

Allen Cell Types Database

TECHNICAL WHITE PAPER: MORPHOLOGY

OVERVIEW

This Technical White Paper describes the histological staining of biocytin filled cells (filled during whole-cell patching of somata and electrical stimulation), their subsequent 20X and 63X bright-field multi-tile, multi-plane imaging, and annotation of the resulting images. High resolution image stacks of biocytin-filled neurons were first evaluated for the likelihood that the morphology will result in a high quality dendritic reconstruction. Three-dimensional (3D) reconstructions of the soma, dendrites and the initial part of the axon were generated for a subset of neurons with a Vaa3D (Peng *et al.*, 2010; Peng, Bria, *et al.*, 2014; Peng, Tang, *et al.*, 2014; Bria *et al.*, 2016) based image processing and reconstruction pipeline starting with a color inversion and a variable enhancement of the signal to noise ratio in the image (Zhou *et al.*, 2014). The enhanced image was then used to generate an automated reconstruction of the neuron with the Neuron Crawler tool (Zhou *et al.*, 2015). The automated 3D reconstructions were then manually corrected and curated and quantitative morphological features were extracted from each final reconstruction file, using other functions of Vaa3D. These features were then used for morphological analyses and biophysical modeling and will provide a foundation for the generation of morphology based taxonomy as well as a synergized analysis and taxonomy with other neuron attributes such as electrophysiology.

HISTOLOGICAL STAINING

DAB Detection of Biocytin Filled Cells

A horseradish peroxidase (HRP) enzyme reaction using diaminobenzidine (DAB) as chromogen was used to visualize the filled cells after electrophysiological recording. The tissue slices containing biocytin filled cells were fixed in 4% paraformaldehyde (PFA) for 16-71 hours at 4°C on an orbital shaker. In the event of an extended weekend, the slices were maintained in 4% PFA for up to 95 hours. The slices were then transferred to 1X Phosphate Buffered Saline (PBS) at 4°C for 1-10 days prior to staining. Slices were rinsed with 1X PBS(+) (1X PBS with 0.0005% Tween-20) three times, incubated in 1% Hydrogen Peroxide (H₂O₂) for 30 minutes to block endogenous peroxidases, and rinsed in 1X PBS(+) another three times. The tissue was then permeabilized with 2% Triton-X 100 in PBS for 60 minutes. Then the slices were incubated for 60 minutes in ABC (Vectastain, Vector Laboratories) at room temperature prior to being stored at 4°C overnight.

After the overnight incubation, slices were incubated for another 60 minutes at room temperature in the ABC reagent. The tissue was then washed with 1X PBS(+) three times prior to visualization of the peroxidase product with a 0.05% DAB, 0.3% H₂O₂, and 1% nickel ammonium sulfate (nickel enhanced DAB) solution. The DAB incubation time was standardized to 1 minute and 45 seconds. After washing the tissue in 1X PBS three times, the slices were fixed with 0.05% osmium tetroxide (OsO₄) in PBS for 60 minutes. This step was designed to reduce tissue shrinkage. Efforts to characterize the extent of shrinkage in X, Y, and Z are in progress. After a final series of three washes in 1X PBS, the tissue slices were mounted on gelatin coated slides and coverslipped with glycerol-based Mowiol mounting media. Slides were dried for approximately 2 days prior to imaging. Mowiol mounting media was made in batches of 100mL and contained: 24g glycerol, 9.6g Mowiol 4-88 (Calbiochem 475904), 24mL MilliQ water, and 48mL 0.2M tris base (pH 8.5). Slides were allowed to dry prior to imaging.

IMAGE ACQUISITION

Mounted sections were imaged on an upright bright-field AxioImager Z2 microscope (Zeiss, Germany) equipped with an AxioCam 506 monochrome camera (6 megapixels with a 4.54 μm per pixel size). Two-dimensional (2D) images were captured with a 20X objective lens (Zeiss Plan-NEOFLUAR 20X/0.5) using the Tile & Position Zeiss Efficient navigation (ZEN) 2012 SP2 software module (Zeiss). Image quality evaluation included a qualitative evaluation of signal to noise for the imaged object (with high signal apparent in the cell body and dendrites, as opposed to background stain in the surrounding tissue, which can occur when cell filling leaks), in-focus cell body, and absent or negligible tessellation (tiling and stitching edge artifact). Overall evenness of section illumination and bounding box region for target tissue inclusion was evaluated.

Individual cells were imaged at higher resolution for the purpose of automated and manual reconstruction, quantitation and display. Light was transmitted using an oil-immersion condenser (1.4 NA). Series of 2D images of single neurons were captured with a 63X objective lens (Zeiss Plan APOCHROMAT 63X/1.4 oil), using the Tile & Position and Z-stack ZEN 2012 SP2 software modules (Zeiss). The composite 2D tiled images (X-Y resolution was set to 0.114 x 0.114 micron) were acquired at an interval of 0.28 μm along the Z-axis. Images were exported as 8-bit TIFF. Image series from individual slices or cells were processed and managed via a custom Laboratory Information Management System (LIMS).

Full dynamic range was achieved with a 20 ms exposure time and an optimal TI VIS-LED lamp voltage control adjustment. Tiles were stitched with a minimum of 5% overlap and a 10% maximum shift. Image quality control included a z-stack plane count, a visual check for proper stitching alignment and even illumination throughout the images. 63X Z-stacks were evaluated based on quality metrics that would impact cell reconstruction, as opposed to aesthetic quality, such as image contrast, stitching and other technical errors. Image “flipping” per section (cell volume and depth not exceeding the objective working distance) and the absence of missing and out-of-order image plane sequence were evaluated.

Annotation of 20X and Blockface Images

Images were taken of the blockface of the brain during sectioning and of a whole slice at 20X after histological processing. Both of these images were manually annotated to determine the location of the recorded cell. To do this, the presence of a labeled soma in the 20X image, and a length of pia and white matter above and below the recording location were drawn, as illustrated in **Figure 1**. These annotations were then used to informatically position the recorded cell in the appropriate cortical region and layer within the Allen Mouse Common Coordinate Framework (CCF). Morphological reconstructions were also mapped into the CCF to approximate the laminar distribution of their dendrites and axons within this cortical region. To begin to assess the accuracy of CCF-derived layer placement, a comparison is on-going between CCF-derived and DAPI-based (4',6-diamidino-2-phenylindole), expert-derived layer calls.

In cases in which a biocytin labeled soma was not visible, or there were multiple cells in the 20X image, a 4X image showing the pipette location during ephys recording was consulted to determine the position of the recorded cell. A Photoshop overlay was used to align the 4X and 20X images, and the approximate location of the pipette tip was assumed to be the recording location.

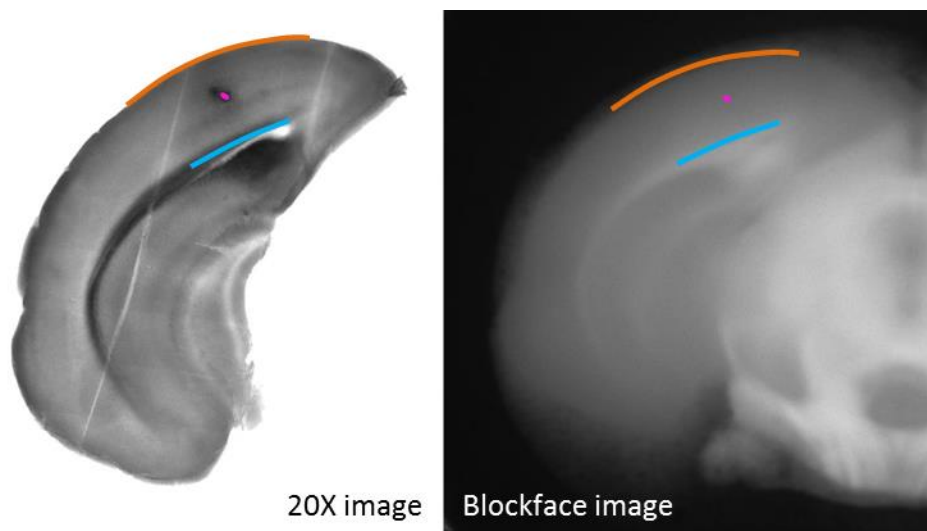


Figure 1. Annotation of recording location (pink), pia (orange) and white matter (blue) on 20X (left) and blockface (right) images. For each recording, matching annotations were drawn on both images to aid in informatics placement of the recording location in the CCF.

Annotation of 63X Images

Following assessment of the quality of the 63X image stack, the soma was manually delineated on a single representative section, providing both a starting point for automated reconstruction and an estimate of soma radius. Each experimental cell was then assessed to determine if a biologically accurate morphological reconstruction could be achieved. Six major categories were evaluated to determine whether a cell would be reconstructed: tissue quality, neurite integrity, neurite fill, extent of non-specific labeling, drying effects and apical dendrite intactness (when applicable).

All quality categories were considered for each cell, and cells with passing scores in all categories were prioritized for morphological reconstruction. A passing score for tissue quality was given if tissue damage did not substantially disrupt the integrity of the dendrites. A passing score for dendritic integrity was given if the majority of its dendrites could be identified as either spiny, sparsely spiny or aspiny (see section below for detailed definitions) and were not abnormally beaded or broken. A passing score for cell fill was given if the majority of dendrites were well labeled, including in the Z dimension. For non-specific labeling, a passing score was given if the soma or dendrites were not obscured by pipette leakage forming a dark “cloud” around the cell, or causing neighboring cells to be stained, obscuring the primary labeled cell. For tissue drying, a passing score was given if the majority of dendrites lacked pronounced tissue drying effects, which can cause the dendrites to appear abnormally kinked or broken. A passing score was given for apical dendrite intactness if the apical dendrite of spiny neurons was contained within the slice all along the length of the primary dendrite. Neurons that met each of these criteria were selected for morphological reconstruction. In some cases, neurons that did not meet these criteria were also reconstructed if the morphology and/or electrophysiology was considered to be sufficiently unique or valuable for understanding cortical cell types.

Morphology Assessment

For the initial data release, the dendritic morphology of each neuron was identified as either aspiny, sparsely spiny or spiny (Braitenberg and Schuz, 1998 with some modification) based on a qualitative assessment of the neuron’s dendrites in the 63X image or by viewing the slides under the microscope. (For future data releases, neuron classification will be further defined as more data are collected.) These different dendritic types roughly equate to interneurons (aspiny and sparsely spiny) and pyramidal or spiny stellate neurons (spiny). It should be noted that individual spines were not reconstructed or quantified in these neurons (methods for quantifying spine density to provide a more quantitative basis for classification into these different categories are being investigated).

Aspiny dendrites were defined by the absence of spiny protrusions, lack of a pronounced apical dendrite and/or axon that emerged from the soma or dendrite at odd angles, and had extensive local branching.

Sparsely spiny dendrites were defined by the presence of infrequent to moderately frequent spiny protrusions (approximately one spine per 10 microns), lack of a pronounced apical dendrite and/or an axon that emerged from the soma or dendrite at odd angles, and had extensive local branching, and /or projected up to layer 1. (*Sparsely spiny neurons were only identified when a 63x image was present.*)

Spiny dendrites were defined by the presence of frequent spiny protrusions (approximately one spine per 1-2 microns), an axon that descended perpendicularly down to the white matter with sparse, proximal branching occurring at right angles to the primary axonal branch and/or a pronounced primary, apical dendrite.

In addition, apical dendrite intactness was categorized for each neuron and defined as the following:

Apical dendrite: A prominent, spiny dendrite that is clearly longer and frequently thicker at its base than all other dendrites. Apical dendrites typically extend toward the pial surface and may or may not end in a tuft.

Intact apical dendrite: An apical dendrite was deemed to be “intact” if the entire length of the *primary* dendritic branch was contained within the thickness of the slice, and was not cut off at either slice surface.

Truncated apical dendrite: An apical dendrite was deemed to be “truncated” if the primary dendritic branch was cut off at either slice surface.

IMAGE PROCESSING AND 3D RECONSTRUCTION OVERVIEW

Microscopy images of single, biocytin-filled neurons were subjected to multi-scale enhancement and automated 3D reconstruction to produce a starting point reconstruction that was then extensively, manually curated and corrected to yield a finalized morphological reconstruction of each neuron. The primary steps are as follows:

1. For an individual cell, stitched, multi-tile, 2D image sequences were color inverted and converted to a single 3D image stack.
2. Image stacks were broken down into individual tiles. An entire set of enhanced 3D image tiles and the tile configuration file were generated by multi-scale image enhancement. The output reconstruction (an SWC file) was produced by Neuron Crawler automatic neuron reconstruction.
3. A refined SWC file was generated by the post-processing step that included short branches pruning and inter-node pruning.
4. The automated reconstruction was manually corrected and curated. This process included deleting false positive branches and connections, adding and extending branches, typing branches (as dendrite or axon), and then connecting the final structure to yield a complete representation of the dendritic and/or axonal tree within the slice.
5. The radius for each neuronal compartment was automatically calculated, checked for accuracy, then manually corrected if necessary.

IMAGE PROCESSING AND 3D RECONSTRUCTION DETAILS

Multi-scale Enhancement

After a cell was selected for reconstruction, the image stack was processed through the informatics pipeline to maximize the signal-to-noise ratio through a customized enhancement. One typical challenge in real world applications of reconstructions is that the input image data may have significant noise and imperfect signal. This phenomenon is particularly pronounced for bright-field images (**Figure 2A**). Direct application of sophisticated automated neuron reconstruction methods to an image with low signal-to-noise ratio (SNR) can yield poor results, such as many of the false branches in an automated 3D reconstruction (**Figure 2B**).

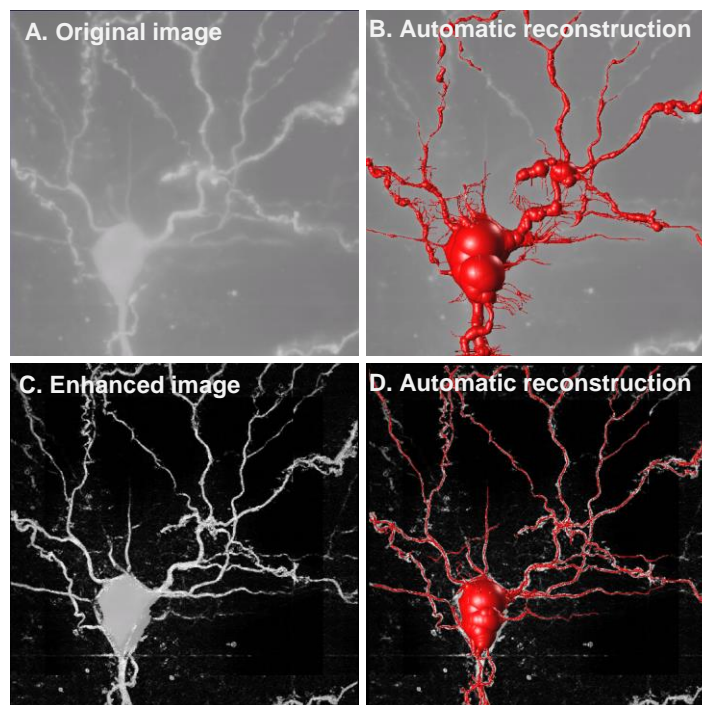


Figure 2. Example bright-field image of a biocytin-filled neuron as well as the enhanced image data and reconstructions.

A. Maximum intensity projections of a bright-field image of a biocytin-labeled mouse neuron. **C.** The enhanced image. **B.** and **D.** Reconstructions (red) produced for both images.

To improve the automatic reconstruction performance (**Figure 2C** and **2D**), a computational method was introduced to enhance the quality of an image that may contain one or more neurons or similar fibrous structures (Zhou *et al.*, 2014). The output of the multi-scale enhancement was an entire set of enhanced 3D image tiles and the tile configuration file that contains the coordinate information.

AUTOMATIC 3D NEURON RECONSTRUCTION

After multi-scale enhancement, an image was then ready for automatic 3D reconstruction. Automatic 3D neuron reconstruction for very large 3D images remains a challenge in neuroscience. Few existing neuron tracing algorithms can be used with commonly available computers (laptops, desktops, or workstations) to efficiently and accurately reconstruct a neuron in large image stacks (>10 GB). Thus, an automatic 3D neuron tracing method called NeuronCrawler was developed (Zhou *et al.*, 2015) (**Table 1**). The key advancement of NeuronCrawler was to trace a small portion of the image first, and then continue to trace only the adjacent tiles where signal was continuous.

Tracing the First Image Tile

NeuronCrawler utilizes a basic tracing method to reconstruct neuronal processes within any of the small image tiles extracted from a large image stack. Many algorithms may be used as the basic tracing module, given that such possible candidates are sufficiently fast and accurate. NeuronCrawler uses All-Path-Pruning 2 (APP2) as the basic tracing module, as APP2 has been shown to be relatively fast and accurate based on pruning a dense initial reconstruction of a neuron to generate a compact representation of the neuron (Peng *et al.*, 2011; Xiao and Peng, 2013).

To avoid extensive computer resources to directly load an entire large 3D image into computer memory, a much smaller 3D image tile was used as the starting location for the reconstruction. The size of such a local region was standardized as $1024 \times 1024 \times N$ (N is the number of z-slices), and the soma, which was manually selected by a human annotator, was used as the starting point for the first round of tracing.

NeuronCrawler

After detecting all terminal tips in the first round of reconstruction, the search continues for potential continuous signal in the adjacent image tiles to grow the neuron structure. This process was iterated until the neuron structure could not be added to any more. In this way, the method works efficiently by tracing only the area with continuous signal. When a boundary terminal tip is used as the new starting location to trace an adjacent image tile, to avoid false continuation and increase the robustness of the tracing, the adjacent tile was required to have 10% overlap with the current tile.

However, the overlapping area between adjacent tiles could cause over-tracing or create topological errors when the reconstructions from adjacent tiles were assembled. To reduce the chance of creating such errors, if the overlap in the reconstruction from two adjacent tiles is greater than 50% then the reconstructions were merged.

The output file of this process was a single SWC file that ranges from roughly 45KB (~1,000 nodes/compartments) to 450KB (~10,000 nodes/compartments).

Table 1. NeuronCrawler algorithm process steps.

Steps	
Input	Soma location, an entire set of 3D image tiles, and the coordinates information.
Step 1	Generate the first 3D image tile using the soma location as the center.
Step 2	Use APP2 to reconstruct the image tile.
Step 3	Check whether or not a terminal tip from the reconstruction is near the boundary. If yes, save it as the new starting location.
Step 4	Use the starting location found in step 3 to reconstruct the adjacent tile with 10% overlap.
Step 5	Fuse the reconstructions from adjacent tiles to avoid over-tracing and topological errors.
Step 6	Iterate process steps 3 to 5, and keep tracing the remaining areas using the boundary tips until no more boundary tips can be found.
Output	Reconstruction result (SWC file).

MANUAL CORRECTION AND CURATION OF THE AUTOMATED 3D RECONSTRUCTION

The automated reconstruction was then extensively manually corrected and curated to provide an accurate representation of the dendrites and either the initial part of the axon or, for a subset of neurons, the full axon within the slice.

Manual reconstruction was performed using the Terafly tools (Bria *et al.*, 2016; Peng, Tang *et al.*, 2014) in Vaa3D (3D Visualization-Assisted Analysis) (www.vaa3d.org) (Peng *et al.*, 2010; Peng, Bria *et al.*, 2014). For this process, the raw (**Figure 3A,B**), raw inverted (**Figure 3C**) and enhanced, inverted (**Figure 3D**) images may all be used. Reconstructions began with an autotrace (described above) (**Figure 3E**). First, false positive branches and connections were removed using the “break and/or delete multiple branches by stroke” tool (**Figure 3F**). The Virtual Finger functions (Peng, Tang *et al.*, 2014) integrated into the Vaa3D platform software were then used for adding and extending branches, particularly dendritic branches (**Figure 3G**). For some axons, which in our dataset commonly appear as a series of regularly-spaced, unconnected puncta, the virtual finger tool may be used to trace branches at the maximum resolution, usually by restricting the visible z-planes to those containing the target process. It is often necessary to simultaneously reference the same image volume in Fiji as a high resolution single plane visual aid. For faint or highly punctate axonal structures, it is necessary to identify the specific z-planes through which the process travels and place nodes at areas of strongest observed signal using the “poly-line” tool (**Figure 3H**). Every attempt was made to generate a completely connected neuronal structure while still remaining faithful to the data. However, if axonal processes cannot be followed

back to an adjacent structure within the same or adjacent planes, they were left unconnected from the remainder of the the axon to provide perspective on axon distribution within the cortex. As a final step in the manual correction and curation processs, another member of the team checks for missed branches or inappropriate connections, and makes adjustments as necessary. Once the reconstruction is complete, multiple plugins may be used to make the appropriate connections between nodes, e.g., “assemble_neuron_live,” “node_connect or neuron_connector.” Other plugins that may be used in the manual reconstruction process include: “typeset_childbranch” and “change nearest neuron segment type by stroke,” which were used to change the branch identity (apical dendrite, basal dendrite and axon); and “linker_file,” which was used to generate terafly compatible SWCs.

Each completed SWC file was then processed through a standardized series of finishing plug-ins. “Sort_neruon_swc_fiji” was used to prepare the SWC for processing by each of the following plug-ins: “Pruning_SWC” was used to remove artifactual short branches introduced by the reconstruction process (<5 nodes). “Resample_SWC” was used to standardize the distance between nodes (step length 10), while also producing a smoothing effect in all three dimensions. “IVSCC_radius_estimation” was used to estimate the radii for every node except the soma (contrast enhanced images were used) (**Figure 3I,J**). A “Slope_analysis” tool was used to assess how dendritic branch radius varied with branch order. Dendrites were observed to be thicker near the soma and thinner at the tips, thus an average negative slope of branch order versus radius was required for a passing radius representation. If a negative slope could not be obtained automatically, a manual radius correction was also performed (**Figure 3J**). (For further information on requirements for radius representation please see the Biophysical Modeling-All Active Technical White Paper in the [Documentation](#) tab.) At this time, no attempt was made to correct artifacts in the radius representation introduced by variation in staining or other methodological issues. Methods for applying an algorithmically derived tapering radius will be tested in the future. For the soma, “Inter_node_pruning” was used to limit the representation of the soma to a single node. “Smooth_SWC” was used to correct the Z-dimension jitter artifact introduced by using virtual finger (serial BBoxes) at high zoom levels on contrast enhanced images (step size 10) (**Figure 3K**). For each reconstruction, quantitative values for morphological features were generated using “Global_neuron_feature.” Dendritic processes that were cut off during slicing or imaging were also indicated as a cut or truncated end by placing an identifying marker at the branch’s terminal node (**Figure 3L**). Axons were treated differently. Only if the axon was cut off very near the soma, was its cut end marked. If the axon continued beyond the proximal soma region, but was not prioritized for reconstruction, it was marked as “continuing” to indicate that there was more to the axon than was represented in the reconstruction. Dendritic processes that did not exit the scanned tissue were left unmarked. The surface of the tissue closest to the soma was also marked. Cut and continuing ends were marked to provide perspective on the intactness of the morphology. In the future, cut end markers may also be used to algorithmically regrow dendritic processes. Cut surface markers may be used to track tissue shrinkage pre- and post-histology.

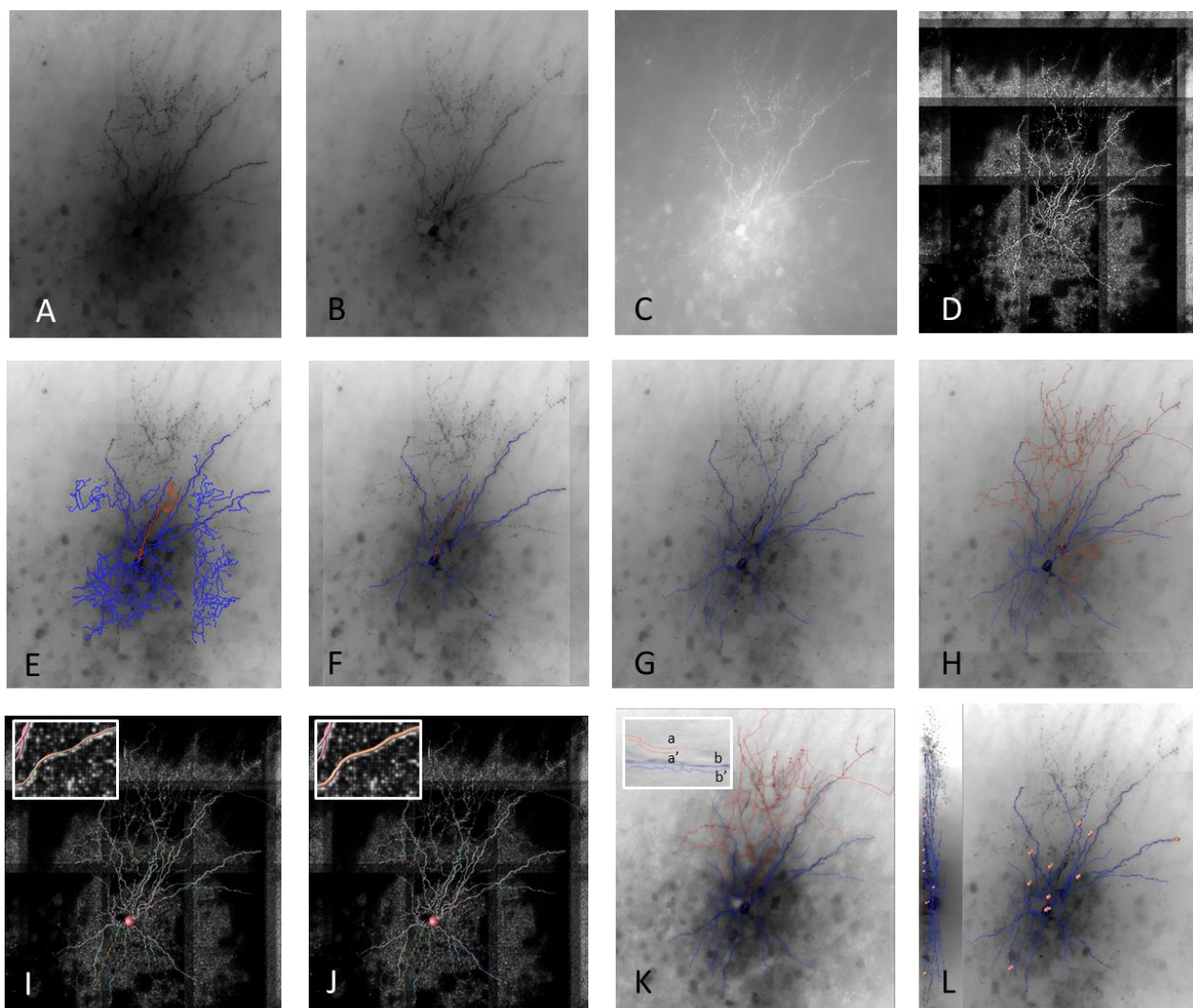


Figure 3. Manual curation and correction of the autotrace using Vaa3D.

Minimum intensity projection (MIP) of the raw 3D image stack (A), after contrast adjustment (B), inverted and adjusted (C), and the inverted enhanced image (D). All of these images may be used during the process of manual correction and curation. Reconstructions began with an autotrace generated based on the enhanced image (described above) (E), false positive branches and connections were then broken and/or deleted. This was then the starting point for the manual reconstruction (F). Dendritic reconstructions were then completed by adding branches using the virtual finger tool in Vaa3D, and connecting branches using the connection and sort plugins (G). Axonal reconstructions were completed by adding axonal branches using the virtual finger and polyline tools (H). Radius was automatically estimated based on the enhanced image and then followed by a branch order vs. radius slope analysis (I). When necessary, automated radius estimation was manually adjusted followed by a branch order vs. radius slope analysis requiring a negative slope be achieved. A negative slope reflected that on average branches were becoming thinner farther from the soma as was observed in the image (J). Branches were smoothed in the z-dimension. Before smoothing a,b and after smoothing a',b' (K). Cut ends of dendritic branches were marked to provide perspective on the intactness of the morphology (L).

Morphology Features

Reconstructions were saved as an SWC file, which is a widely used ASCII format for specifying neuronal morphology (e.g., used by neuromorpho.org (Ascoli *et al.*, 2007)). Multiple morphological features were then extracted from the final reconstructions. Extracted features will provide a foundation for the generation of morphology based taxonomy as well as a synergized analysis and taxonomy with other neuron attributes such as electrophysiology.

Extracted features included twenty-one global morphology metrics. A subset of morphology features defined in L-Measure (<http://cng.gmu.edu:8080/Lm/help/index.htm>) (Scorcioni *et al.*, 2008) were produced in the informatics pipeline by the Vaa3D plugin “Compute Global Features” (**Table 2**). To see descriptive images of the Morphology Features (except number of nodes) for dendrites only, hover over the name to follow the hyperlink embedded in the text.

Table 2. Global morphology features.

Morphology Features	Definition
Number of nodes	The total number of nodes in the given input neuron (one SWC file). A node in a SWC file represents a single sample point of the neuron defined by its X, Y and Z coordinates, a radius, and its connectivity to other nodes in the neuron.
Soma surface area	The surface of the soma is computed by one of two methods. If the soma is composed of just one node then the sphere assumption is used; otherwise the sum of the external cylindrical surfaces of nodes forming the soma is calculated.
Number of stems	The number of stems attached to the soma. When the type of the node is not soma, it is labeled as a stem.
Number of bifurcations	The number of bifurcations for the given input neuron. A bifurcation point has two daughters.
Number of branches	The number of branches in the given input neuron. A branch is one or more compartments that lie between two branching points or between one branching point and a termination point.
Number of tips	The number of terminal tips for the given input neuron. This function counts the number of nodes that are terminal endpoints.
Neuronal height	Height is computed on the y-coordinates and it is the difference of minimum and maximum y-values after eliminating the outer points on either end by using the 95% approximation of the y-values of the given input neuron.
Neuronal width	Width is computed on the x-coordinates and it is the difference of minimum and maximum x-values after eliminating the outer points on either end by using the 95% approximation of the x-values of the given input neuron.
Neuronal depth	Depth is measured on the y-coordinates and it is the difference of minimum and maximum y-values after eliminating the outer points on either ends by using the 95% approximation of the y-values of the given input neuron.
Average diameter (thickness)	The average diameter of all compartments of the neuron.
Total length	The total length of the neuron is computed as the sum of distances between two connected nodes for all branches of the input neuron.
Total surface area	The total surface area of the entire neuron.
Total volume	The total volume of the entire neuron.
Maximum Euclidean distance to root	The maximum Euclidean distance of all nodes. Euclidean distance is the straight line distance from the soma (root) to the node.

Maximum path distance to root	The maximum path distance of all nodes. The path distance is the sum of lengths of all connected nodes from the soma, ending with that node.
Maximum branch order	The maximum order of the branch. A branch's order is defined with respect to the soma where the soma has a branch order = 0. The first bifurcation has a branch order = 1, the second bifurcation has a branch order = 2, and so on.
Average contraction	The average ratio between Euclidean distance of a branch and its path length. Euclidean distance of a branch is the straight-line distance from the soma to the branch. Path length is the sum of the lengths between each node along the path.
Average fragmentation	The average number of compartments that constitute a branch between two bifurcation points or between a bifurcation point and a terminal tip.
Average parent-daughter ratio	The average ratio between the diameter of a daughter branch and its parent branch. One value for each daughter branch is generated at each bifurcation point.
Average local amplitude angle	The average angle between the first two compartments (in degree) at a bifurcation.
Average remote amplitude angle	The average angle between two bifurcation points or between bifurcation point and terminal point or between two terminal points.

REFERENCES

- Ascoli GA, Donohue DE, Halavi M (2007) NeuroMorpho.Org: a central repository for neuronal morphologies. *Journal of Neuroscience* 27:9247-9251.
- Braitenberg V and Schuz A (1998) *Cortex: Statistics and Geometry of Neuronal Connectivity*. Second Edition. Springer-Verlag Berlin Heidelberg, New York.
- Bria A, Iannello G, Onofri L, Peng H (2016) TeraFly: real-time 3D visualization and annotation of terabytes of multidimensional volumetric images. *Nature Methods* (in press).
- Dong HW (2008) *Allen Reference Atlas: A Digital Color Brain Atlas of the C57BL/6J Male Mouse*. Hoboken, NJ: John Wiley & Sons.
- Paxinos G, Franklin KBJ (2001) *The Mouse Brain in Stereotaxic Coordinates*, Second Edition. Elsevier Academic Press, San Diego, CA.
- Peng H, Ruan Z, Long F, Simpson JH, Myers EW (2010) V3D enables real-time 3D visualization and quantitative analysis of large-scale biological image data sets. *Nature Biotechnology* 28:348-353.
- Peng H, Long F, Myers G (2011) Automatic 3D neuron tracing using all-path pruning. *Bioinformatics* 27:i239-i247.
- Peng H, Bria A, Zhou Z, Iannello G, Long F (2014) Extensible visualization and analysis for multidimensional images using Vaa3D. *Nature Protocols* 9:193-208.
- Peng H, Tang J, Xiao H, Bria A, Zhou J, Butler V, Zhou Z, Gonzalez-Bellido PT, Oh SW, Chen J, Mitra A, Tsien RW, Zeng H, Ascoli GA, Iannello G, Hawrylycz M, Myers E, Long F (2014) Virtual finger boosts three-

dimensional imaging and microsurgery as well as terabyte volume image visualization and analysis. *Nature Communications* 5:4342.

Scorcioni R, Polavaram S, Ascoli GA (2008) L-Measure: a web-accessible tool for the analysis, comparison and search of digital reconstructions of neuronal morphologies. *Nature Protocols* 3:866-876.

Xiao H, Peng H (2013) APP2: automatic tracing of 3D neuron morphology based on hierarchical pruning of a gray-weighted image distance-tree. *Bioinformatics* 29:1448-1454.

Zhou Z, Sorensen S, Zeng H, Hawrylycz M, Peng H (2014) Adaptive Image Enhancement for Tracing 3D Morphologies of Neurons and Brain Vasculatures. *Neuroinformatics* 1-14.

Zhou Z, Sorensen S, Peng H (2015) Neuron crawler: an automatic tracing algorithm for very large neuron images. *Proceedings of IEEE 2015 International Symposium on Biomedical Imaging: From Nano to Macro*, 870-874.